https://doi.org/10.48047/AFJBS.6.15.2024.1698-1718

African Journal of Biological Sciences

Journal homepage: http://www.afjbs.com

Research Paper Open Access

Design, Synthesis, and biological evaluation of isocryptolepine derivatives: SAR of indolo [3, 2-c] quinoline as anti-oxidants and anti-tyrosinase agents

Shourya Pratap[a,*], AbhilashaMittal[a], Sambit Kumar Parida[b]

[a]*Institute of Pharmacy, NIMS University Rajasthan, Jaipur*

[b]*Institute of Pharmacy, AMITY University Rajasthan, Jaipur*

***Corresponding Author:** Mr. Shourya Pratap, Research Scholar, Institute of Pharmacy, NIMS University Rajasthan, Jaipur

Email- shouryayadav122@gmail.com

Volume 6, Issue 15, Sep 2024

Received: 15 July 2024

Accepted: 25 Aug 2024

Published: 05 Sep 2024

doi: 10.48047/AFJBS.6.15.2024.1698-1718

Abstract

Objectives: This study aims to create 3D QSAR models to confirm the antioxidant and anti-tyrosinase activity of indolo[3,2-c] quinoline analogs and determine nearly all appreciative structural features in contemplation of developing novel medicinal medicines.

Methods: To appraise predicted precision of the QSAR framework, the datasets were split into a training set and test set. The training set encompasses 39 analogs, chosen randomly, whereas the test set comprised 10 analogs. The chemicals were selected to guarantee a variety of structures and a broad spectrum of biological effects in the dataset. The IC_{50} values were transformed into pIC_{50} to get higher numerical values.

Results: The cross-validated r^2 (q^2) values for the training set of 39 analogs in the CoMFA, CoMSIA, & HQSAR models are 0.470, 0.572, and 0.639, respectively. Conversely, the conventional r^2 values for the identical models are 0.982, 0.809, and 0.960. A total of 49 derivatives of the indolo [3, 2-c] quinoline core were expose to docking and QSAR analyses. The final results act as a prototype for the development of a chemical compound that is more powerful in combating oxidative stress.

Conclusion: The utilization of 3D-QSAR models, in conjunction with the inventive incorporation of contour maps and chemical descriptors, presents new ideas and methods for the creation of indolo [3, 2-c] quinoline analogs with antioxidant and antityrosinase properties.

Keywords: QSAR, HQSAR, Docking, Antioxidant activity, Antityrosinase activity.

1. Introduction:

Antioxidants are substances that prevent oxidation, a chemical process that can generate free radicals and trigger cascading reactions that may harm cells.[1-4] They have a crucial function in the prohibition on cancer, cardiovascular, as well as neurological disorders.[5-6] Excessive tyrosinase activity and the presence of oxidative stress are associated with several diseases and skin conditions characterized by oxidative damage. As a result, they are considered potential targets for treatment approaches.[7-10] Oxidative stress is characterized by the

dysregulation of RNS and ROS. Furthermore, these species not only induce cellular and molecular damage but also disrupt normal physiological processes and detoxification mechanisms.[11-12] ROS and RNS free radicals are responsible for several health conditions such as cataracts, cancer, and neurodegenerative diseases.[13-15] Oxidative stress is associated with over 100 diseases and has negative effects on aging, imbalances in physiological function, the development of further diseases, and human lifespan.[16-17] Antioxidants, obtained from both natural and artificial sources, have effectively been used to decrease the production of free radicals and protect the body's detoxifying mechanisms.[18-20] RNS and ROS free radicals, such as O_2, H_2O_2, HO, and NO, are involved in avoiding damage according to references.[21-23] Antioxidants are efficacious remedies for conditions associated with oxidative stress due to their ability to function as reducing agents or radical scavengers.[24-25] They halt chain reactions by scavenging various free radicals generated during oxidative processes.[26-27] The bulk of synthetic antioxidants now available on the market consist of heterocyclic and polyphenolic chemicals.[28-29] By utilizing insilico design procedures on this nucleus,[30-31] there is a notable probability of generating novel and captivating organisms. One widely used method for assessing the impact of different molecule fragments and characteristics on biological activity is the quantitative structure-activity relationship (QSAR).[32-33] Various descriptors, including hydrophobic, steric, electrostatic, donor, and acceptor, are used in 3D QSAR (CoMFA and CoMSIA) to create statistical models.[34-35] The HQSAR fragment differentiation map provides a good illustration of the robust statistical correlation between biological activity and structure. This fragmentation map provides information about the contributions made by different structural components to activity.[36-37] Docking studies elucidate the interconnection allying ligand & the active site of the macromolecular protein, revealing the molecular basis of binding affinity and specificity. By utilizing different amino acid binding's necessary for a physiological response, we can evaluate interactions between enzymes and ligands at the molecular level.[38-39]

2. Materials and methods:

A dataset of 49 indolo[3, 2-c]quinoline analogs to conduct docking studies, revealing the molecular basis of binding affinity and specificity, and their corresponding biological activity was obtained from previous publications N. Wang et al., 2014.[40] The Chemdraw Ultra Version 8.0 program is used to create 2D structures, which are then converted into 3D Chemdraw Ultra Version 8.1 models using MOPAC. SYBYL 2.0 is used for CoMFA, CoMSIA, and HQSAR models, while SYBYL 2.1 is used for docking studies. The training set consists of 39 compounds, while the test set contains 10 compounds. Table 1 also displays the structures of all the substances under investigation accompanied by the biological data where applicable.

Table 1: Residual values of training and test set of molecules of the CoMFA, CoMSIA and HQSAR model.

Compound Number	Actual pIC_{50}	CoMFA		CoMSIA		HQSAR A/B/Ch/D	
		Predicted pIC_{50}	Residual value	Predicted pIC_{50}	Residual value	Predicted pIC_{50}	Residual value
1	4.991	5.1217	-0.1307	5.3606	-0.3696	5.02852	-0.03752
2	7.8633	7.6635	0.1998	7.3607	0.5026	7.75807	0.10523
3	7.4425	7.6471	-0.2046	7.584	-0.1415	7.48026	-0.03776
4*	7.8996	7.7293	0.1703	7.7016	0.198	7.451	0.4486
5	7.8239	7.7957	0.0282	7.7996	0.0243	7.41139	0.41251
6	7.5784	7.7392	-0.1608	7.8173	-0.2389	7.70755	-0.12915
7	7.1993	7.2175	-0.0182	7.2443	-0.045	7.14355	0.05575
8	8.0269	7.6884	0.3385	7.7738	0.2531	7.8794	0.1475
9	6.852	6.8786	-0.0266	6.7139	0.1381	6.9152	-0.0632

10	6.6449	7.0356	-0.3907	7.2286	-0.5837	7.14354	-0.49864
11	6.9454	6.9497	-0.0043	6.8916	0.0538	6.76758	0.17782
12	7.7305	7.4773	0.2532	7.3829	0.3476	7.82539	-0.09489
13	6.4994	6.5832	-0.0838	6.3431	0.1563	6.47631	0.02309
14*	7.8861	7.6904	0.1957	7.3717	0.5144	7.489	0.3971
15	8.0915	7.6881	0.4034	7.3628	0.7287	7.68653	0.40497
16	7.4425	7.6413	-0.1988	7.4529	-0.0104	7.6491	-0.2066
17*	8.2076	7.6347	0.5729	7.3499	0.8577	7.603	0.6046
18	7.5302	7.5812	-0.051	7.6105	-0.0803	7.58891	-0.05871
19	7.5935	7.5731	0.0204	7.7806	-0.1871	7.47109	0.12241
20	7.6556	7.7472	-0.0916	7.5728	0.0828	7.74001	-0.08441
21*	7.6289	7.9545	-0.3256	7.1685	0.4604	8.094	-0.4651
22	8.6198	8.1842	0.4356	7.8157	0.8041	8.0938	0.526
23	7.5901	7.5033	0.0868	7.7174	-0.1273	7.69779	-0.10769
24*	6.5396	7.7828	-1.2432	7.7247	-1.1851	7.746	-1.2064
25	7.6478	7.6586	-0.0108	7.8852	-0.2374	7.89492	-0.24712
26	7.6271	7.9024	-0.2753	7.9668	-0.3397	7.98483	-0.35773
27	7.767	7.8302	-0.0632	7.5497	0.2173	7.94927	-0.18227
28	7.6162	7.4923	0.1239	7.7603	-0.1441	7.52303	0.09317
29	7.5686	7.8557	-0.2871	7.8073	-0.2387	7.81153	-0.24293
30	7.9626	7.839	0.1236	7.7866	0.176	7.87949	0.08311
31	7.9747	8.0013	-0.0266	7.9991	-0.0244	7.904	0.0707
32*	7.2652	7.4174	-0.1522	7.7023	-0.4371	7.359	-0.0938
33	7.1427	7.3313	-0.1886	7.1109	0.0318	6.87815	0.26455
34*	7.3862	7.6133	-0.2271	7.5479	-0.1617	8.123	-0.7368
35	7.1403	7.2878	-0.1475	7.4763	-0.336	7.13718	0.00312
36	5.1316	4.8368	0.2948	5.1884	-0.0568	5.1583	-0.0267
37	7.1409	7.2545	-0.1136	7.1	0.0409	7.26311	-0.12221
38*	6.5627	7.2144	-0.6517	7.457	-0.8943	7.131	-0.5683
39	7.0306	7.2705	-0.2399	7.4816	-0.451	7.24409	-0.21349
40	7.5045	7.3055	0.199	7.1485	0.356	7.43991	0.06459
41	7.2343	7.3233	-0.089	7.4984	-0.2641	7.30787	-0.07357
42	7.3134	7.2859	0.0275	7.5452	-0.2318	7.42089	-0.10749
43	7.451	7.2861	0.1649	7.1416	0.3094	7.32305	0.12795
44	7.0205	7.301	-0.2805	7.4759	-0.4554	7.19101	-0.17051
45	7.3883	7.2489	0.1394	7.5208	-0.1325	7.30403	0.08427
46	7.2782	7.2553	0.0229	7.098	0.1802	7.2312	0.047
47	7.5031	7.2814	0.2217	7.2098	0.2933	7.25571	0.24739
48*	7.4828	7.155	0.3278	7.1214	0.3614	7.083	0.3998
49*	8.1367	7.324	0.8127	7.3265	0.8102	7.471	0.6657

(*) test compounds

2.1 Structural alignment:

The molecular modeling studies, were conducted using SYBYL X 2.0 software. The compound structures were energy minimized utilizing Tripos energy shield and Gasteiger-Huckel charges, Convergence was determined at 0.05 kcal/mol, ideally based on CoMFA and CoMSIA.[40-41] Crucially, for both CoMFA and CoMSIA, primary requirement is superimposition of all 3D structures, ideally based on a pharmacophore in its active conformation.

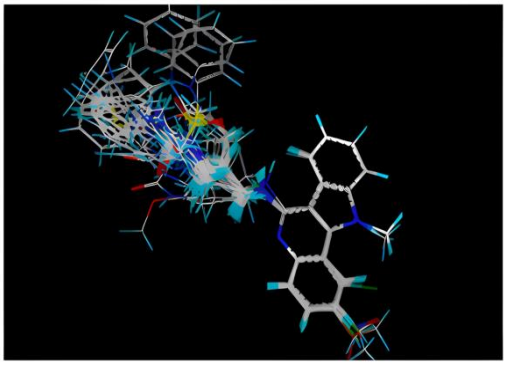

Figure 1: Structure alignment of all indolo [3, 2-c] quinoline analogues

3. Experiment:

3.1 CoMFA and CoMSIA statistical results:

CoMFA employed to establish a correlation link chemical structure and biological activity of a compound, it consist of contour maps representing the interaction energies of a probe atom with aligned molecules.[42-47] The steric and electrostatic probable fields were generated at each intersection of a square grid of 2.0 Å for the selected compounds significant biological characteristics.[48-53] CoMFA & CoMSIA incorporates a Gaussian-type function to model distance dependence of physicochemical properties.[54-55] Several factors such as coefficient of determination (r^2), cross-validated coefficient of determination (q^2), and standard error of estimation are used to construct the QSAR model. To establish the external predictability, the Leave-One-Out (LOO) cross-validation was used as a method, and from this also emerged the cross-validated r^2 (q^2) and the number of components.[56-57] The best CoMFA & CoMSIA models were obtained using the Gasteiger charge as the almost comparable charge, yielding the q^2 values of 0.470 and 0.572 respectively. As for the results of the CoMFA & CoMSIA analyses, the values of the coefficient of determination (r^2) were equal to 0.982 and 0.809, respectively. The CoMFA steric field contribution was 0, implying that again the feasibility of the compound alternatives is not influenced by steric hindrance factors. 485, meanwhile the electrostatic field's contribution was 0.515. This indicates that the electron-donating as well as electron-withdrawing groups are prominent in the activity. Thus, in CoMSIA analysis, better statistical results are obtained regarding the cross-validated r^2 (or q^2). CoMSIA analysis examines more fields than the CoMFA analysis, while the choice of these fields is carried out according to certain criteria.[58-59] The CoMSIA study described steric and electrostatic fields and hydrophobic and donor fields also. These are highlighted in table 2 below. The steric, electrostatic, hydrophobic, and donor fields of the best CoMSIA model have contributions of 0.313, 0.037, 0.080, and 0.570, respectively.

Table 2: Summary of statistical results of best CoMFA and CoMSIA models.

QSAR	Parameters					Contributions			
	q^2	r^2	NC	F-value	SEE	S	E	H	D
CoMFA	0.470	0.982	6	135.931	0.078	0.485	0.515	-	-
CoMSIA	0.572	0.809	1	84.051	0.222	0.313	0.037	0.080	0.570

q^2 is Cross validated r^2, NC is Number of Components, SEE is Standard error of estimate, S-Steric , E-Electrostatic, H-Hydrophobic and D-H bond donor.

3.2 CoMFA Steric and Electrostatic Contour Map Analysis:

The presence of a green contour around the substituted side chain connected to the pyridine ring of the quinoline skeleton suggests the need for a large group to enhance antioxidants and anti-tyrosinase activity in the nitrogen of the indole ring and the phenyl ring of the quinoline moiety. Never the less, the presence of a yellow contour above the phenyl ring connected to the terminal end of the substituted side chain signifies that the addition of any large group nearby will certainly reduce the antioxidants and anti-tyrosinase activity. In the CoMFA electrostatic field contour, regions with higher electronegativity that enhance binding affinity are depicted in red, while regions with higher electropositivity that enhance binding affinity are depicted in blue. Figure 2 illustrates these interactions.

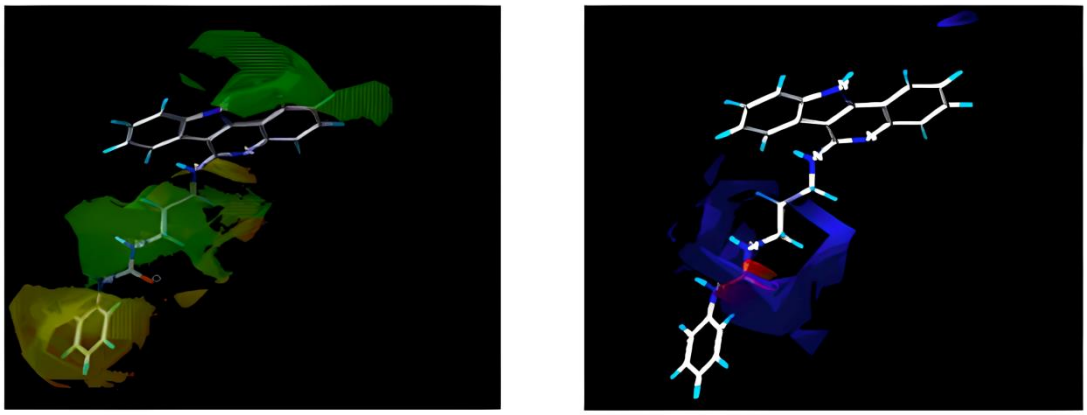

a. Steric contour **b. Electrostatic contour**

Figure 2: CoMFA Steric and Electrostatic contour map analysis molecule 22.

3.3 CoMSIA Steric, Electrostatic, HB Accepter, HB Donor, and Hydrophobic contour:

The green contour map in CoMSIA steric analysis represents advantageous spatial arrangements for bulky groups, whereas the yellow contour indicates non-tolerant positions for such groups. The green contour above the phenyl ring of the quinoline structure and around the substituted side chain indicates the need for a large group to enhance antioxidants and anti-tyrosinase activity. The electrostatic field contour map shows regions where electronegative groups enhance binding affinity, while electropositive groups enhance binding affinity. The magenta contour near the urea attachment site indicates the need for hydrogen bond acceptor (HB-acceptor) groups, while the cyan contour near the urea group indicates the need for hydrogen bond donor (HB-donor) groups. Figure 3 illustrates these interactions.

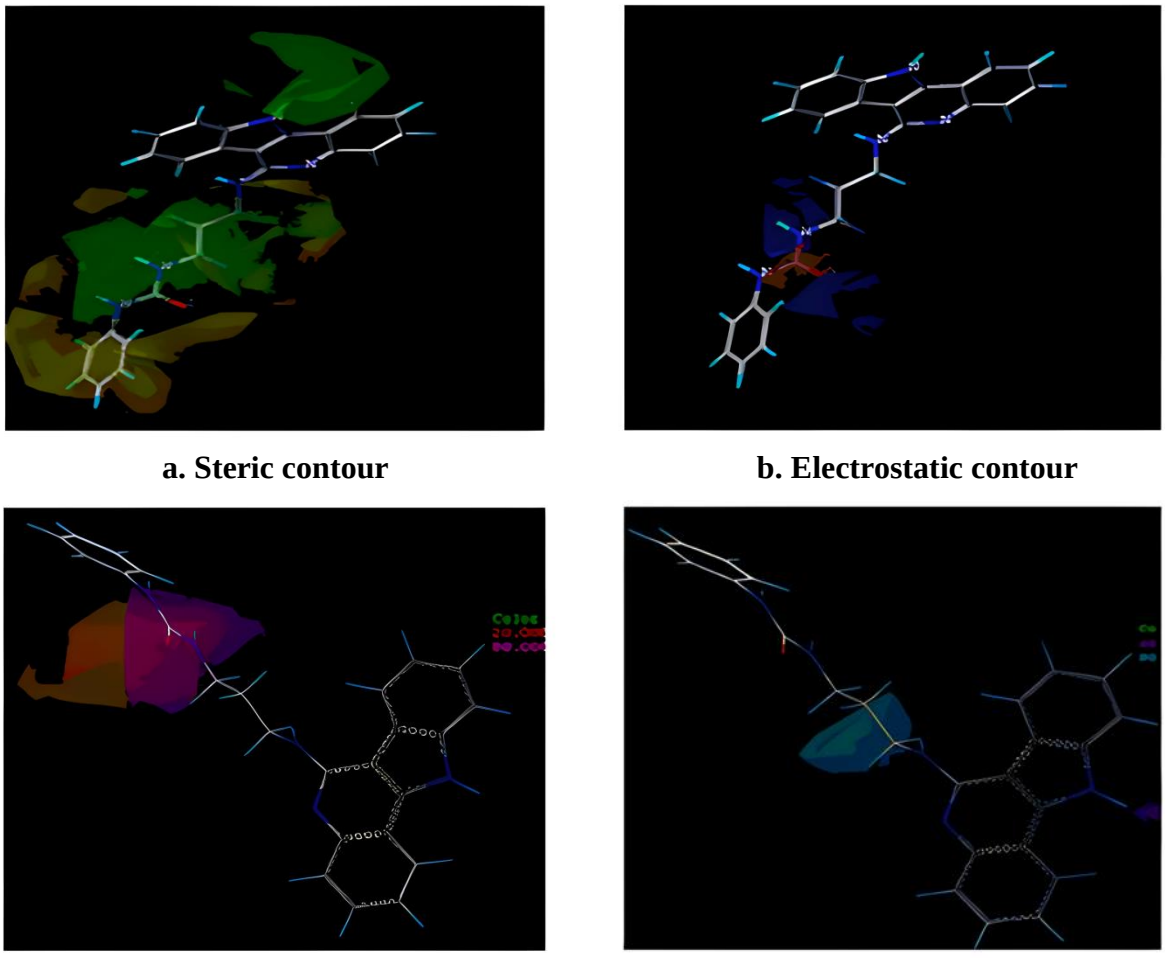

a. Steric contour **b. Electrostatic contour**

c. HB Accepter **d. HB Donor**

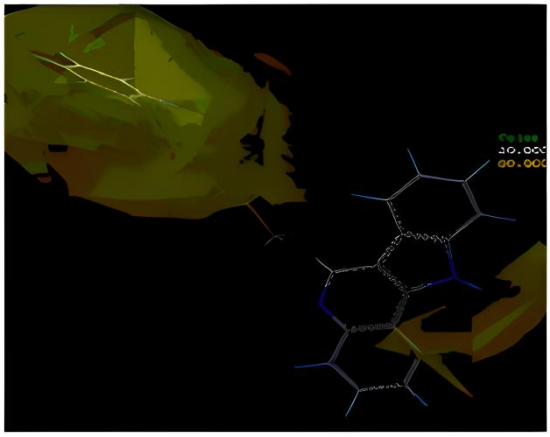

e. Hydrophobic

Figure 3: CoMSIA Steric, Electrostatic, HB Accepter, HB Donor, and Hydrophobic contour molecule 22.

3.4 HQSAR analysis:

2D QSAR approaches utilize various atomic fragments such as atoms, bonds, and connections in the form of a molecular hologram to establish correlations between the pharmacological actions of substances. This technique possesses a distinctive characteristic that allows for the examination of the individual contribution of each molecule being studied to the biological activity. The fragment distinctions were employed using various fragment sizes to facilitate the construction of the model.[60-61] The statistical analysis shows that the model development yields the best results when using a distinct A/B/Ch/D fragment with a size ranging from 4 to 8 fragments, as shown in Table 3.

Table 3: A/B/Ch/D fragment distinct with different fragment sizes.

Model No.	Fragment Size	q^2	r^2	Q^2 S.E.	r^2 S.E.	Ensemble	Best length	N.C
1	2-5	0.679	0.912	0.292	0.172	0.912	199	6
2	3-6	0.655	0.928	0.311	0.161	0.928	199	6
3	4-7	0.632	0.950	0.322	0.134	0.950	199	6
4	5-8	0.635	0.961	0.330	0.119	0.961	199	6
5	6-9	0.520	0.962	0.378	0.118	0.962	199	6
6	7-10	0.402	0.976	0.422	0.093	0.976	199	6
7	2-6	0.652	0.929	0.312	0.161	0.929	199	6
8	3-7	0.623	0.950	0.326	0.134	0.950	199	6
9	**4-8**	**0.639**	**0.960**	**0.328**	**0.120**	**0.960**	**199**	**6**
10	5-9	0.536	0.962	0.372	0.118	0.962	199	6
11	6-10	0.420	0.977	0.416	0.091	0.977	199	6

3.5 HQSAR contour analysis:

The HQSAR analysis of compound number 22 reveals a green contour at the urea replacement of the terminal phenyl ring, indicating a beneficial influence on the antioxidants and anti-tyrosinase activity (see Figure 4).

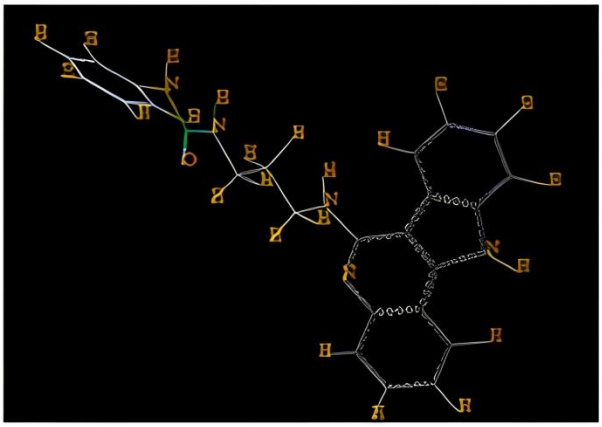

Figure 4: HQSAR fragment contribution in most active compound 22.

3.6 Docking analysis:

The Surflex Dock module of SYBYL X 2.1 is used here in molecular docking investigations. The rationale for using docking was to obtain the probable binding orientations of the indole [3, 2-c] quinoline derivatives with the receptor. The crystal structure of mushroom tyrosinase (PDB ID: 2Y9X Human serotonin 5-HT7 receptor structure was downloaded from the Protein Data Bank of the RCSB and was used as the docking template.[62-65] The terminal structure was energy minimized, and charges were calculated in the AMBER7FF99 method. Subsequently, the intended complex protein structure was utilized to assess and validate the docking technique. The protein, ligands, and solvation water molecules were removed from the crystal structure. The protocol was configured with a bloat value of 1 and a threshold value of 0.5. The active receptor binding sites were identified based on the positions considered in Table 4 and binding biological activity, as seen in Figure 5.

Table 4: Docking score of Compounds on 2Y9X.

S. No.	Compound No.	Total Score	S. No.	Compound No.	Total Score
1	5	8.55	**25**	19	6.36
2	23	8.49	**26**	43	6.36
3	48	8.26	**27**	17	6.27
4	38	8.11	**28**	8	6.16
5	47	8.01	**29**	18	6.04
6	40	7.89	**30**	14	6.03
7	20	7.76	**31**	31	5.94
8	37	7.74	**32**	34	5.91
9	3	7.67	**33**	29	5.76
10	33	7.59	**34**	45	5.67
11	49	7.5	**35**	46	5.62
12	26	7.49	**36**	16	5.62
13	41	7.28	**37**	35	5.61
14	15	7.22	**38**	42	5.55
15	25	7.13	**39**	39	5.39
16	4	7.11	**40**	44	5.3
17	10	7.06	**41**	11	5.08
18	2	7.04	**42**	24	5.06
19	6	6.94	**43**	7	5
20	30	6.91	**44**	21	4.71
21	27	6.84	**45**	13	4.62
22	28	6.77	**46**	9	4.24
23	32	6.69	**47**	12	3.85
24	22	6.54	**48**	36	2.58

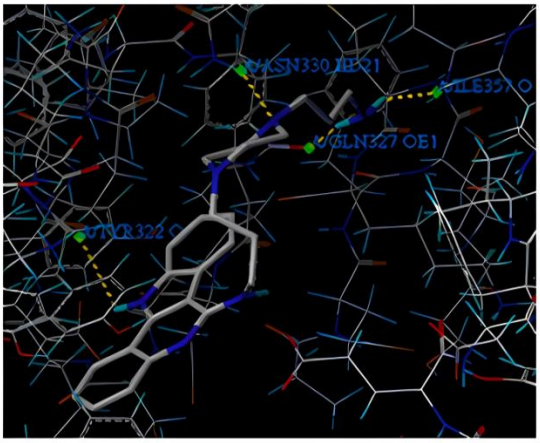

a. Compound 5

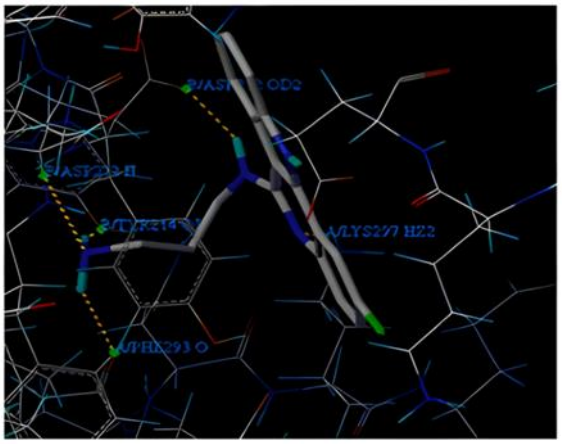

b. Compound 23

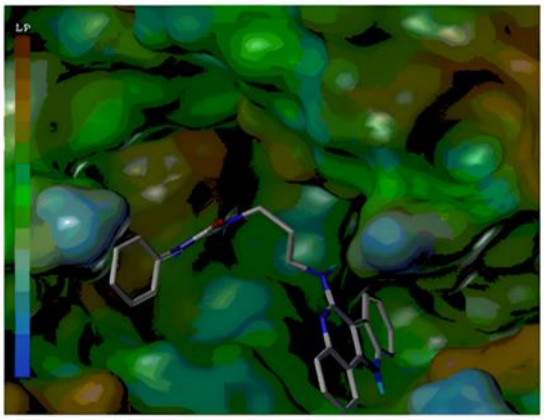

a. Compound 5 lipophilic interaction

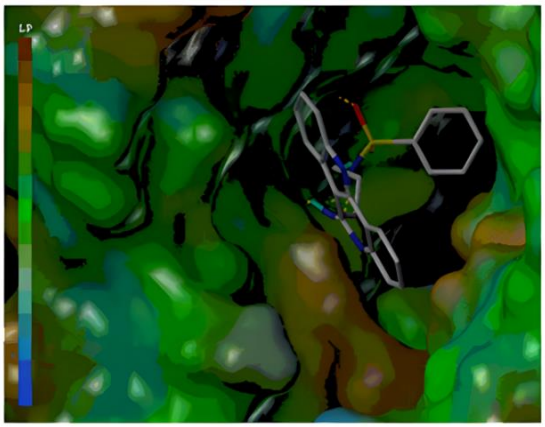

b. Compound 23 lipophilic interaction

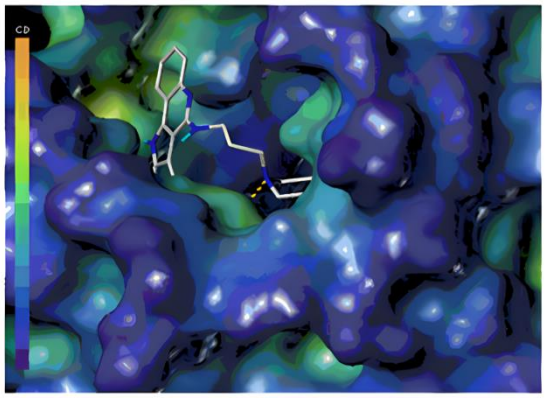

a. Compound 5 cavity depth view

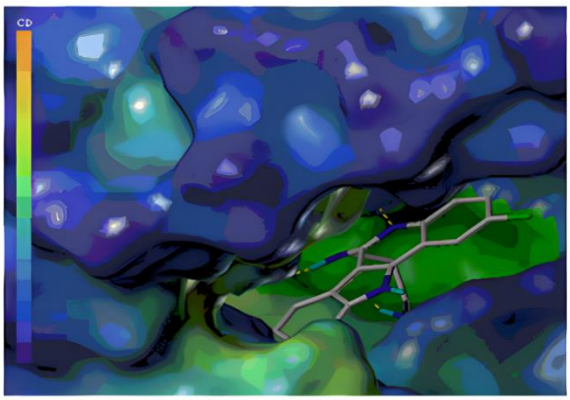

b. Compound 23 cavity depth view

3.7 Designing of compounds:

Based on the documented association between the structure and activity of indole [3, 2-c] quinoline analogs as antioxidants and anti-tyrosinase agents, we conducted QSAR research using CoMFA, CoMSIA, HQSAR, and Docking techniques. We created and analyzed thirty compounds, as presented in Table 5. The outcome confirmed the SAR acquired in the investigation depicted in Figure 6.

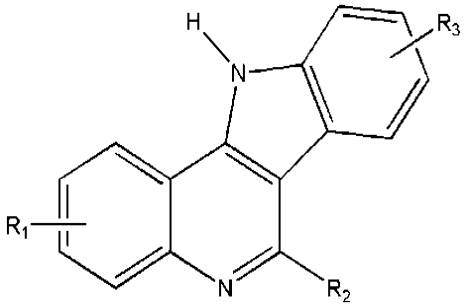

Figure 6: Designed compound with different substitution at R_1, R_2 and R_3 Position.

Table 5: The structures and predicted pIC_{50} values of designed derivatives.

C. N.	Substituents			Pred pIC_{50}			
	R1	R2	R3	CoMFA	CoMSIA	HQSAR	Docking Score
1	7-Chloro	Methylamino	Chloro	6.8522	6.0315	7.643	7.83
2	7-Chloro	N-methyl piperazino	Chloro	6.7931	5.9774	8.529	8.40
3	7-Chloro	N-ethyl piperazino	Chloro	6.7886	5.933	8.609	6.71
4	7-Chloro	Benzyl amino	Chloro	6.8674	6.5704	7.914	5.92
5	7-Chloro	N-butyl amino	Chloro	6.8199	6.4092	7.724	4.42
6	Methoxy	N-Hydrogen	Hydoxyl	6.6508	5.6205	8.056	7.01
7	7-Chloro	3-hydroxy aniline	Chloro	6.9484	6.6479	7.397	7.12
8	7-Chloro	4-hydroxy aniline	Chloro	6.9597	6.5336	7.51	6.53
9	7-Chloro	4-bromo aniline	Chloro	6.922	6.4537	6.972	8.12
10	7-Chloro	2,3 dichloro aniline	Chloro	7.2207	6.6878	6.868	5.12
11	7-Chloro	2-nitro aniline	Chloro	7.2969	6.6612	6.869	3.45
12	7-Chloro	4-fluro aniline	Chloro	6.9697	6.3577	6.978	3.94
13	7-Chloro	3-chloro aniline	Chloro	7.0951	6.6701	7.559	5.12
14	7-Methyl	Methylamino	Chloro	6.7292	5.8543	7.648	6.32
15	7-Methyl	N-methyl piperazino	Chloro	6.6365	5.8718	8.534	3.14
16	7-Methyl	N-ethyl piperazino	Chloro	7.2135	6.0927	8.614	7.18
17	7-Methyl	Benzyl amino	Chloro	6.7666	6.5202	7.919	8.14
18	7-Methyl	N-butyl amino	Chloro	6.6241	6.2255	7.732	7.49
19	7-Methyl	4-(3-amino propylmorpholino)	Chloro	6.6046	5.5994	8.06	6.35
20	7-Methyl	3-hydroxy aniline	Chloro	6.819	6.4798	7.402	7.96
21	7-Methyl	4-hydroxy aniline	Chloro	6.8468	6.4276	7.515	7.69
22	7-Methyl	4-bromo aniline	Chloro	6.7718	6.3227	7.054	5.32
23	7-Methyl	2,3 dichloro aniline	Chloro	7.0359	6.5145	6.95	3.32
24	7-Methyl	2-nitro aniline	Chloro	7.0603	6.5919	6.952	4.34
25	7-Methyl	4-fluro aniline	Chloro	6.9576	6.4757	7.061	4.35
26	5-Ethoxy	3-hydroxy aniline	Chloro	7.6258	7.2641	7.449	7.14
27	5-Ethoxy	4-hydroxy aniline	Chloro	7.6068	7.1671	7.562	4.81
28	5-Ethoxy	4-bromo aniline	Chloro	7.7858	7.277	7.118	5.94
29	5-Ethoxy	2,3-dichloro aniline	Chloro	7.9243	7.2907	7.014	6.06
30	5-Ethoxy	2-nitro aniline	Chloro	8.0938	7.4107	7.016	4.06

3.8 Synthetic scheme:

Bergman's 2003 method for synthesizing 5, 11-dehydroindolo[3,2-c]quinoline-6-one using isatin and 2-aminobenzylamine.[66] All the reagents were used without any additional purification, using commercially available reagents. The synthesis of Isatin involved introducing M-anisidine, m-taurolidine, and 3-chloroaniline into a flask, followed by adding water and strong hydrochloric acid. Two solutions were added, one containing anhydrous sodium sulfate and chloral hydrate, and the other hydroxylamine hydrochloride. The mixture was heated to 100^0C for 6 hours, then cooled and dissolved in sodium hydroxide. The solid

components were collected, washed and dried. The chlorination of 2-AminoBenzylamine involved a mixture of methanol and water, treated with dilute hydrochloric acid, and extracted with dichloromethane. The synthesis of intermediates involved a mixture of Chlorinated Aminobenzylamine and substituted Isatin, which was heated and refluxed for 17 hours. Dehydrative chlorination with POCl3 was conducted, and amino groups were added to the carbon atom at position 13 using an ArSN reaction using various amines, as shown in Figure 7.

2a. 3-(4-(3,8-dichloro-11*H*-indolo[3,2-*c*]quinoli-6-yl)morpholin-2-yl)propan-1-amine: Yield 22.9%, M.P. 70 ± 3˚C, Rf value 0.6 cm^{-1}, FTIR (cm^{-1}) C-Cl stretch- 505.70, 602.32,N-H stretch- 3270.65, N-H bend-1559.44,O-H stretch 3600.75,Aromatic C sp^2-3006.62, ^{1}H NMR (δppm) A ring: 5.0-7.0 (1H,3CH), C ring: 9.83 (1H, 1NH), D ring: 5.0-8.2 (1H,3CH), E ring: 2.05-4.6 (1H,3CH_2), F: 2.05-2.53 (1H, 3CH_2), G: 2.04 (1H, 1NH_2), ^{13}CNMR A ring: 126.32-157.10, B ring: 112.82-169.79, C ring: 137.64, D ring: 110.68-111.81, E ring: 38.28-38.68, F (aliphatic chain): 23.70, MASS(m/z) 429 [M^+].

2b. 8-chloro-3-methyl-6-(4-methylpiperazin-1-yl)-11*H*-indolo[3,2-*c*]quinoline Yield 24.9%, M.P. 87 ± 3˚C, Rf value 0.7 cm^{-1}, FTIR (cm^{-1}) C-Cl stretch- 565.59, 709.76.N-H stretch- 3304.13,C (sp2)-H stretch- 3093.65, ^{1}H NMR (δppm) A ring: 2.28-2.33 (3H,1CH_3), E ring: 2.05-3.73 (1H,4CH_2), F(CH_3): 2.05-2.54 (3H,1CH_3), ^{13}CNMR A ring CH_3: 21.05, B ring: 168.39-172.08, E ring: 53.40-53.78, F (CH_3): 44.31-44.41, MASS(m/z) 294.

2c. 8-chloro-6-(4-ethylpiperazin-1-yl)-3-methyl-11*H*-indolo[3,2-*c*]quinoline Yield 40.9%, M.P. 93 ± 3˚C, Rf value 0.9 cm^{-1}, FTIR (cm^{-1}) C-Cl stretch- 776.78,N-H bend- 1514.50, Alkanes-C-H stretch- 2816.36, 2880.49,CH3 bend- 1371.78, ^{1}H NMR (δppm) A ring: 2.26-2.99 (1H,1CH_3), E ring: 2.5-4.5 (1H,4CH_2), F: 1.23-1.77 (1H,1C_2H_5), ^{13}CNMR A ring CH_3: 22.56-29.05, B ring: 168.93, E ring: 38.12-40.07, F (CH_3CH_2): 13.47-13.62, MASS(m/z) 392.

2d. *N*-benzyl-8-chloro-3-methyl-11*H*-indolo[3,2-c]quinolin-6-amine Yield 22.9%, M.P. 87 ± 3˚C, Rf value 0.4 cm^{-1}, FTIR (cm^{-1}) C-Cl stretch- 618.14, Aromatic C=C stretch-1463.87,C(sp2)-H stretch- 3187.63, ^{1}H NMR (δppm) A ring: 7.10-7.49(1H,3CH), 2.28-2.54(1H,1CH_3), C ring: 8.45(1H,1NH), D ring: 7.10-7.49 (1H,3CH) E: 3.98 (1H,NH), F: 4.22-4.68(1H,1CH_2), G ring: 7.10-7.49 (1H,5CH), ^{13}CNMR A ring: 139.43-159.49, A ring CH_3: 17.52-22.47, B ring: 169.50, C ring: 133.95, D ring: 116.30-133.95, E: 40.17-42.21, F ring: 126.35-139.43, MASS(m/z) 389.7.

2e. *N*-butyl-8-chloro-3-methyl-11*H*-indolo[3,2-c]quinolin-6-amine Yield 45.9%, M.P. 53 ± 3˚C, Rf value 0.6 cm^{-1}, FTIR (cm^{-1}) C-Cl stretch- 756.53,Alkane CH3 bend- 1443.62,N-H bend- 1575.25, 1598.88,N-H stretch- 3367.48, 3381.95,Asym.CH3 stretch- 2973.51, ^{1}H NMR (δppm) A ring: 2.05-2.74(1H,1CH_3), E: 4.67-4.72 (1H,1NH), F: 1.11-3.07 (1H,C_4H_9), ^{13}CNMR A ring: 126.36-131.53, A ring CH_3: 21.01, B ring: 116.25-172.00, C ring: 131.53, D ring: 79.22-131.53, E (aliphatic chain): 10.20-51.07, MASS(m/z) 298.7.

2f. 4-methoxy-11*H*-indolo[3,2-c]quinoline-8,9-diol Yield 85%, M.P. 95 ± 3˚C, Rf value 0.7 cm^{-1}, FTIR (cm^{-1}) OCH_3 2786, OH 3348 ^{1}H NMR (δppm) 6.70–6.85 (d, 2H, Ar-H), 9.8 (s, H, NH), 8.94 (s, 1H, Ar-H), 6.93-7.38 (t, 3H, Ar-H), 3.78 (s, 1H, OCH) ^{13}C NMR (δppm)A ring: 131.0-135.2, B ring: 127.8-128.7, C ring: 125.5-119.0, D ring: 114.3-111.1, 55.8 (OCH_3). MASS (m/z) 198.80 [M+].

2g. Ethyl 8-fluoro-11,11a-dihydro-11-methyl-6a*H*-indolo[3,2-c]quinoline-6-carboxylate Yield: 38%, M.P. 61± 3˚C, Rf value 0.8 cm^{-1}, FTIR (cm^{-1}) N–CH_3 2752, C = O 1498-1589, ^{1}H NMR (δppm) 6.9–8.2 (m, 7H, Ar-H), 4.4 (q, 2H, CH_2), 4.0 (s, 3H, N–CH_3), 3.9 (t,

3H, CH_3), ^{13}C NMR (δppm) 168.2 (C O), 149.9 (C–F), 154.5(C= O), A ring: 128.1-131.2, B ring: 121.9-130, C ring: 114.8-121.8, D ring: 108.5-120.0, 69.1 (CH_2), 41.2 (N–CH_3), 15.3 (CH_3); MASS (m/z) 319.

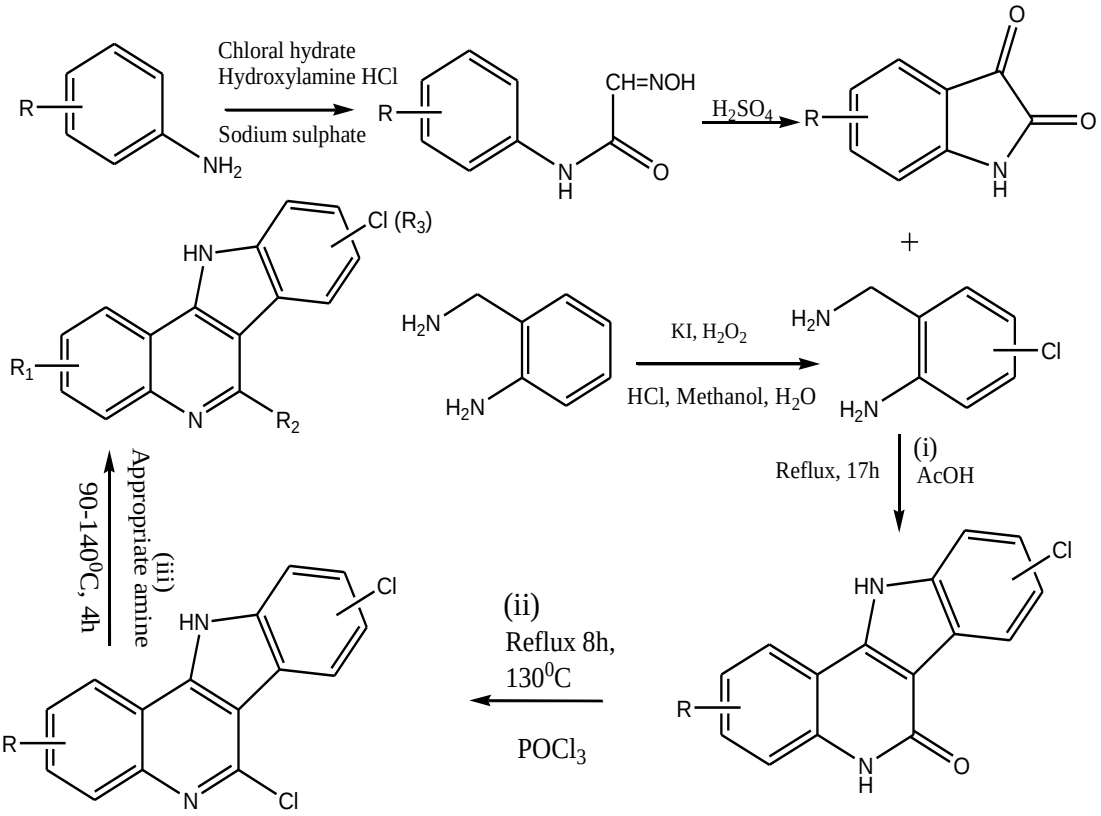

Figure 7: Synthetic scheme isocryptolepine derivatives

2h. 11-bromo-6-ethyl-6, 11-dihydro-8-methoxy-5-methyl-5*H*-indolo[3,2-c]quinoline Yield: 62%, M.P. 98 ± 3˚C, Rf value 0.7 cm^{-1}, FTIR (cm^{-1}) N–CH_3 2761, C= O 1553-1744, ^1H NMR (δppm) 6.65–7.30 (m, 7H, Ar-H), 4.5 (q, 2H, CH_2), 4.1 (q, 2H, CH); 3.73 (s, 3H, OCH_3), 2.83 (s, 3H, N–CH_3), ^{13}C NMR (δppm) C-O 160.1, A ring: 110.2-129.7 B ring: 60.6-138.5 C ring: 112-119 D ring: 102.1-155.6, 65.3(CH_2), 55.7 (OCH_3), 35.5 (N–CH_3). MASS (m/z) 404 [M^+]

2i. 11-fluoro-2-iodo-11*H*-indolo[3,2-c]quinoline-8-ol Yield: 62%, M.P. 68 ± 3˚C, Rf value 0.2 cm^{-1}, FTIR (cm^{-1}) I 1357, N-F 1048, O-H 1340, ^1H NMR (δppm) 7.69–8.22 (t, 3H, Ar-H), 7.99 (s, H), 6.1-7.2 (t, 2H, CH); 5.07 (s, H, OH), ^{13}C NMR (δppm) A ring: 110.2-139.1 B ring: 119.8-148.6 C ring: 135.1-132.9 D ring: 117.1-152.6, MASS (m/z) 279.71.

2j. 9-bromo-6,11-dihydro-5-methyl-11-nitro-5*H*-indolo[3,2-c]quinoline-6-ol Yield: 62%, M.P. 64 ± 3˚C, Rf value 0.2 cm^{-1}, FTIR (cm^{-1}) CH_3 bend 1405, O-H 3670- 3578, Br 686-510, NO2 1651, ^1H NMR (δppm) 6.66–7.31 (t, 3H, Ar-H), 5.64 (s, H), 6.9-7.6 (t, 3H, CH); 2.37 (s, H, OH), ^{13}C NMR (δppm) A ring: 110.3-138.8 B ring: 123.1-85.6 C ring: 139.1-123.9 D ring: 115.9-140.3, MASS (m/z) 299.21 [M+2].

2k. 11-bromo-3-(trifluoromethyl)-6, 11-dihydro-5*H*-indolo[3,2-c]quinoline-9-ol Yield: 69%, M.P. 101± 3˚C, Rf value 0.4 cm^{-1}, FTIR (cm^{-1}) O-H 3198, Br 689, CF_3 1301, ^1H NMR (δppm) 5.8–7.4 (t, 3H, Ar-H), 4.7 (s, H), 3.5-4.13 (d, 2H, Ar-H); 5.57-6.94 (t, H, Ar-H), ^{13}C NMR (δppm) A ring: 94.9-146.9 B ring: 117.4-126 C ring: 58.6-112.9 D ring: 108.1-150.2, MASS (m/z) 381.6.

2l. 11-bromo-11,11a-dihydro-9-hydroxy-6a*H*-indolo[3,2-c]quinoline-3-carboxylic acid Yield: 78%, M.P. 99 ± 3˚C, Rf value 0.8 cm^{-1}, FTIR (cm^{-1}) O-H 3234, Br 843, COOH 3298, ^1H NMR (δppm) 4.89–5.99 (t, 3H, Ar-H), 4.8 (s, H), 4.1-4.27 (t, 3H, Ar-H); 7.32-8.18 (t, H,

Ar-H), ^{13}C NMR (δppm) A ring: 98.3-156.5C ring: 58.1-163.7 D ring: 122.2-141.8, C chain: 169.4MASS (m/z) 365.74.

2m. 11-bromo-11,11a-dihydro-3-(nitromethyl)-6a*H*-indolo[3,2-c]quinoline-9-ol Yield: 48%, M.P. 108± 3˚C, Rf value 0.3 cm^{-1}, FTIR (cm^{-1}) O-H 3401, Br 736, NO_2 1493, ^{1}H NMR (δppm) 6.08–6.78 (t, 3H, Ar-H), 5.7 (s, OH), 3.4-7.58 (t, 3H, Ar-H); 7.12-7.61 (t, H, Ar-H), ^{13}C NMR (δppm) A ring: 101.1-166.1 C ring: 71.7-168.1 D ring: 123.1-138.1, C chain: 79.2 MASS (m/z) 298.76.

2n. 3-amino-5-(9-chloro-4-ethoxy-11*H*-indolo[3,2-c]quinoline-6-yl)phenol Yield: 68%, M.P. 110 ± 3˚C, Rf value 0.8 cm^{-1}, FTIR (cm^{-1}) O-H 3287, NH2 1575, Cl 757, C-O 1598, CH3 1482, ^{1}H NMR (δppm) 7.40–7.87 (t, 3H, Ar-H), 9.1 (s, NH), 5.89-6.78 (t, 3H, Ar-H); 5.02-6.31 (t, H, Ar-H), 5.73 (s, OH), 1.30-4.08 (d, CH2) 6.05 (s, NH2), ^{13}C NMR (δppm) A ring: 124.1-171.0 B ring: 119.1-137.8, C ring: 144.9-161.3 D ring: 117.8-147.5, E ring: 102.7-149.1 Co chain: 17.1, MASS (m/z) 319.42 [M+2].

2o. 2-amino-4-(9-chloro-4-ethoxy-11*H*-indolo[3,2-c]quinolin-6-yl)phenol Yield: 46%, M.P. 123 ± 3˚C, Rf value 0.5 cm^{-1}, FTIR (cm^{-1}) O-H 3312, NH2 1564, Cl 621, C-O 1645, CH3 1396, ^{1}H NMR (δppm) 6.78–7.49 (t, 3H, Ar-H), 9.8 (s, NH), 5.75-7.62 (t, 3H, Ar-H); 5.59-6.9 (t, H, Ar-H), 5.12 (s, OH), 2.18-3.87 (d, CH3) 3.85 (s, NH2), ^{13}C NMR (δppm) A ring: 117.9-136.9 B ring: 121.3-138.2C ring: 142.1-159.0 D ring: 121.1-145.5, E ring: 131.2-146.2 Co chain: 17.8-64.8, MASS (m/z) 278.32 [M+].

2p. 3,4-dichloro-5-(9-chloro-4-ethoxy-11*H*-indolo[3,2-c]quinoline-6-yl)benzenamine Yield: 76%, M.P. 168 ± 3˚C, Rf value 0.6 cm^{-1}, FTIR (cm^{-1}) NH2 1391, Cl 674, C-O 1476, CH3 1389 ^{1}H NMR (δppm) 6.78–7.81 (t, 3H, Ar-H), 8.7 (s, NH), 7.12-7.67 (t, 3H, Ar-H); 5.71, 6.95 (d, 2H, Ar-H), 2.12-3.79 (d, CH3) 4.09 (s, NH2), ^{13}C NMR (δppm) A ring: 123.7-135.7 B ring: 123.0-141.8, C ring: 141.3-157.1 D ring: 131.0-149.7, E ring: 116.2-148.0 Co chain: 16.1-63.7, MASS (m/z) 321.20.

4. Results and discussion

Emanate from the SAR and docking studies generated through molecular modeling analysis, 30 novel antioxidants were auspiciously crafted, showing promising speculated activities across computational avenue. Subsequently, 16 of the top compounds were synthesized to evaluate their antioxidant and anti-tyrosinase activities in vitro.

4.1 In vitro antioxidant activities

Four different types of antioxidant assay methods viz. DPPH, Hydrogen peroxide, and superoxide assay define the radical scavenging ability of synthesized compounds and FRAP activity measures the reducing capacity of the synthesized compounds. All the compounds found good statistical correlation and the activities are reported in Table 6.

a) DPPH scavenging activity

The experiment evaluated substances' antioxidant capacity by measuring their ability to eliminate or neutralize free radicals. The compound 1, 1-diphenyl-2-picrylhydrazyl (DPPH) was used as the radical.[67-68] Synthesized substances were prepared at various concentrations and tested in a test tube. A control solution, BHT, was used as a positive control. The absorbance was measured at a wavelength of 517 nm using a UV-visible spectrophotometer.[69] All the synthesized compounds manifest a various degree of DPPH scavenging action with IC_{50} values ranging from 183.42µg/ml and 893.31µg/ml. 2f (IC_{50} 183.42 ± 1.4µg/ml) displayed activity comparable with BHT (IC_{50} 171.11± 0.51µg/ml). The antioxidant activity of 2f may be because of the presence of electron-donating hydroxyl and methoxy substituent on the phenyl ring. 2m (IC_{50} 210.13 ± 0.59µg/ml) also displayed activity

comparable with BHT because of the presence of methyl and hydroxyl electron-donating substituent. Other synthesized compounds 2e, 2g, 2i, 2j, 2k, 2l, 2o, and 2p with IC_{50} values 463.92, 331.53, 480.71, 392.73, 250.53, 529.64, 213.13µg/ml also show good scavenging activity. The descending order of activity is-

BHT>2f>2m>2o>2k>2h>2g>2p>2j>2n>2e>2i>2l> 2c>2b>2d>2a

b) FRAP assay

This technique converts ferric ions into ferrous ions under acidic conditions. A test tube contains TPTZ solution, FeCl3 solution, and synthesized chemicals. Absorption at 593 nm is measured after 30 minutes, with a control without synthesized ingredients. The absorbance of the synthesized compounds was compared to standard absorbance (BHT).[70-71] Results convey that 2f exhibited potential reducing power with an EC_{50} of 220.09 ± 0.74µg/ml which is almost equal to standard BHT (223.03 ± 1.3µg/ml). Besides 2f other compounds 2k (293.32± 0.17µg/ml), 2m (312.11 ± 0.22µg/ml), and 2o (252.05 ± 0.27µg/ml) also show good activity. The descending order of activity is-

2f>BHT>2k>2g>2m>2h>2p>2i>2n>2j>2o>2e>2d>2l>2c>2a>2b

c) Hydrogen peroxide (H_2O_2) scavenging assay

The scavenging activity involves converting hydrogen peroxide into water. A 40 mM solution was prepared, mixed with synthesized compounds, and measured at wavelength of 230 nm. A control was prepared using hydrogen peroxide without any synthesized chemicals.[72-73] None of the synthesized compounds tested here are more active than BHT concerning hydrogen peroxide scavenging. 2f (IC_{50} 172.24 ± 0.53µg/ml) displayed activity comparable with BHT (140.4 ± 1.7µg/ml). This is because of the presence of hydroxyl and methoxy groups (electron-donating substituent) on the terminal phenyl ring.

BHT>2f>2o>2m>2k>2g>2j>2p>2h>2i>2n>2l>2d>2e>2a>2c>2b

d) Superoxide (SOD) radical scavenging activity

The superoxide radical assay measured the antioxidant's ability to prevent NBT reduction in an alkaline DMSO solution, prepared by mixing nitroblue tetrazolium and synthesized chemicals. The absorbance at 560 nm was measured after 10 minutes.[74-77] The most active compound 2f (IC_{50} 193.49 ± 0.86µg/ml) having 2-hydroxyl and 4-methoxy substituent on the phenyl ring displayed activity comparable with BHT (IC_{50} 207.6 ± 0.97µg/ml). 2k, 2m and 2o (IC_{50} 253.50, 329.43, and 252.35 µg/ml respectively) displayed activity comparable with BHT (IC_{50} 207.6 ± 0.97µg/ml).

2f>BHT>2o>2k>2h>2m>2j>2g>2p>2i>2n>2d>2l>2c>2e>2b>2a

Table 6: Antioxidant activities of synthesized indolo [3, 2-c] quinoline derivatives

S. No.	DPPH (IC_{50}, µg/ml)	FRAP (EC_{50}, µg/ml)	H_2O_2 (IC_{50}, µg/ml)	Superoxide (IC_{50}, µg/ml)
2a	893.31±0.9***	972.7±0.45***	872.07±0.7***	913.72±0.5***
2b	657.5±0.6***	1013.32±0.4***	913.04±0.7***	862.73±0.55***
2c	641.40±1.8***	893.09±0.47***	907.90±0.6***	819.5±0.65***
2d	676.7±1.2***	752.37±1.2***	810.39±0.8***	772.06±0.75***
2e	463.92±0.71***	620.02±0.7***	817.29±0.6***	840.45±0.65***
2f*	183.42±1.4***	220.09±0.7ns	172.24±0.5***	193.49±0.86***
2g	331.53±2.3***	302.09±0.7***	313.35±2.2***	345.34±0.95***
2h	293.39±0.74***	330.32±0.5***	352.05±0.5***	310.95±0.45***
2i	480.71±0.83***	454.07±1.3***	395.09±0.6***	445.72±1.73***

2j	392.73±1.4***	551.07±0.7***	325.45±0.9***	344.07±0.59***
2k	250.53±0.62***	293.32±0.6***	295.23±0.7***	253.50±0.66***
2l	529.64±0.74***	752.67±0.9***	767.52±0.9***	804.02±0.79***
2m	210.13±0.59***	312.11±0.8***	287.75±0.6***	329.43±0.75***
2n	410.35±0.72***	512.29±0.7***	529.12±0.6***	515.55±0.65***
2o	213.13±0.59***	252.05±0.6***	220.13±0.7***	252.35±0.95***
2p	352.01±0.67***	352.29±1.9***	331.02±1.3***	352.47±0.85***
BHT	171.11±0.71	223.03±0.76	140.4±1.7	207.6±0.97

*****p<0.0001 (significantly different from standard)**
ns- not significantly different from standard

4.2 Tyrosinase Inhibition Assay

The tyrosinase inhibitory activity was assessed using the modified dopachrome technique.[78-79] Synthesized compounds were created in a solution containing 50% DMSO. The absorbance was quantified at a wavelength of 475 nm, with kojic acid serving as the positive control. The results were compared to a control group where 50% of DMSO was used instead of the synthesized molecule.[80-81] 2f (IC_{50} 123.49 ± 0.86 µg/ml) displayed antityrosinase activity comparable with Kojic acid (IC_{50} 90.21± 1.2 µg/ml). 2a was showing very weak antityrosinase activity (IC_{50} 913.72 ± 0.5).

Table 7: Antityrosinase activities of IPH6 and IPH15

S. No.	Compound ID	Antityrosinase activity (IC_{50} µg/ml)
1.	**2f**	123.49 ± 0.86 *******
2.	**2a**	413.72 ± 0.5*******
3.	**Kojic acid (Standard)**	90.21±1.2

*****p<0.0001(significantly different from standard)**

5. Conclusion:

This work aimed to develop 2D and 3D QSAR relationship of indolo[3, 2-c]quinoline derivatives by parameters. The aim stood in fact, to establish the relationship that exists between the structures of these analogs and their therapeutic effect. The final conception was to obtain information for designing enhanced antioxidants and potential inhibitors against tyrosinase. Results CoMFA, CoMSIA, and HQSAR revealed significance result concerning internal validation (q2) for indolo[3,2-c]quinoline derivatives. By comparing the q2 values obtained by different QSAR techniques, it can be stated that we have designed three rational and reasonable QSAR models. While CoMFA pinpointed advantageous and disadvantageous fields, the models of CoMSIA rendered information about the advantageous field and disadvantageous fields respectively. Similarly, the model of HQSAR provided details of positive field, negative field and intermediate field concerning the sub-structural fingerprint needs to impact on biological activity. According to the flexible docking methodology, the binding mode of the indole [3,2-c] quinoline analogs was predicted. Further, it was concluded that HBD interactions are significant for the stability of protein on PDB 2Y9X during the binding process. This information is essential to understanding the manner and conditions that are necessary for the formation of certain biological outcomes. Laboratory experiments showed that all the synthesized indolo[3, 2-c]quinoline derivatives proved to have high antioxidant and antityrosinase activity. Across all the assays and between them, the levels of activity differed. Similarly, in the DPPH assay, it was found that IC_{50} was 183.42 ± 1.4µg/ml.

In the experience with the FRAP assay, the EC_{50} was close to the decrease in IC50 of the standard drug which was 220.09 ± 0.74µg/ml. In the H_2O_2 scavenging assay all the synthesized compounds had less activity than the BHT standard but compound 2f had almost similar activity. The obtained value of the IC_{50} for compound 2f in the SOD radical scavenging assay is 172.24 ± 0 of successfully tested concentrations, the studied substance proved to be more active with an IC_{50} value of 53µg/ml, while the standard has an IC_{50} value of 193.49 ± 0.86µg/ml.

Conflict of interest:

The authors assert that no competing interests exist.

Acknowledgements:

I would like to thank Prof. Gopal Natesan (Director, Institute of Pharmacy, Nirma University Ahmedabad, Gujarat) for providing me with the resources to conduct molecular modeling studies.

List of abbreviations:

CoMFA: comparative molecular field analysis, **CoMSIA:** comparative similarity indices analysis, **HQSAR:** Hologram quantitative structure-activity relationship, **PLS:** Partial least-squares, **PRESS** is the sum of squares of the prediction errors, $\mathbf{q^2}$: Predictive squared correlation coefficient, $\mathbf{r^2}$**:** Non-cross-validated correlation coefficient, **F**: Yields to optimistic predictive abilities, $\mathbf{IC_{50}}$**:** Half-maximal inhibitory concentration, $\mathbf{pIC_{50}}$**:** Negative log of the IC_{50} value when converted to molar, **SE:** Standard error, **HB:** Hydrogen bond, **ROS:** Reactive oxygen species, **RNS:** Reactive nitrogen species, $\mathbf{O_2}$**:** Oxygen, $\mathbf{H_2O_2}$**:** Hydrogen peroxide, **HO:** Hydroxide, **NO:** Nitrous oxide, **BHT:** Butylated hydroxyl toluene, **DPPH:** 2,2-Diphenyl-1-picrylhydrazyl, **TPTZ:** 2,4,6-Tripyridyl-s-triazine, **NBT:** Nitro blue tetrazolium chloride, **DMSO:** Dimethyl sulfoxide, **FRAP:** Ferric reducing antioxidant power, **A/B/C/H/Ch/DA** Atoms/bonds/connections/hydrogen atoms/ chirality/donor, acceptor.

References:

1. Chaudhary P, Janmeda P, Docea AO, Yeskaliyeva B, Abdull Razis AF, Modu B, Calina D. Oxidative stress, free radicals and antioxidants: Potential crosstalk in the pathophysiology of human diseases. Front. in Chem. 2023; 11: 1158198. https://doi.org/10.3389/fchem.2023.1158198

2. Lobo V, Patil A, Phatak A, Chandra N. Free radicals, antioxidants and functional foods: Impact on human health. Pharmacogn. Rev. 2010; 4(8): 118–126. https://doi.org/10.4103/0973-7847.70902

3. Silva SAME, Michniak-Kohn B, Leonardi G.R. An overview about oxidation in clinical practice of skin aging. An. Bras. Dermatol. 2017; 92(3): 367–374. https://doi.org/10.1590/abd1806-4841.20175481

4. Tan BL, Norhaizan ME, Liew WP, Sulaiman Rahman H. Antioxidant and Oxidative Stress: A Mutual Interplay in Age-Related Diseases. Front. pharmacol. 2018; 9: 1162. https://doi.org/10.3389/fphar.2018.01162

5. Martemucci G, Costagliola C, Mariano M, Napolitano P, Gabriella A. Free Radical Properties, Source and Targets Antioxidant Consumption and Health. Oxygen. 2022; 2(2): 48-78. https://doi.org/10.3390/oxygen2020006

6. Olufunmilayo EO, Michelle B, Holsinger RM. Oxidative Stress and Antioxidants in Neurodegenerative Disorders. Antioxidants, 2023; 12(2): 517. https://doi.org/10.3390/antiox12020517

7. Eskandani M, Golchai J, Pirooznia N, Hasannia S. Oxidative stress level and tyrosinase activity in vitiligo patients. Indian J. Dermatol. 2010; 55(1): 15–19. https://doi.org/10.4103/0019-5154.60344
8. Popoola OK, Marnewick JL, Rautenbach F, Ameer F, Iwuoha EI, Hussein AA. Inhibition of Oxidative Stress and Skin Aging-Related Enzymes by Prenylated Chalcones and Other Flavonoids from Helichrysum teretifolium. Molecules. 2015; 20(4): 7143–7155. https://doi.org/10.3390/molecules20047143
9. Zengin G, Mahomoodally MF, Picot-Allain CMN, Cakmak YS, Uysal S, Aktumsek A. In vitro tyrosinase inhibitory and antioxidant potential of Consolida orientalis, Onosma isauricum and Spartium junceum from Turkey. S. Afr. J. Bot. 2019; 120: 119-123. https://doi.org/10.1016/j.sajb.2018.01.010.
10. Moon KM, Yang J, Lee M, Kwon E, Baek J, Hwang T, Kim J, Lee B. Maclurin Exhibits Antioxidant and Anti-Tyrosinase Activities, Suppressing Melanogenesis. Antioxidants. 2022; 11(6): 1164. https://doi.org/10.3390/antiox11061164
11. Sandalio LM, Collado-Arenal AM, Romero-Puertas MC. Deciphering peroxisomal reactive species interactome and redox signalling networks. Free Radic. Biol. Med. 2023; 197: 58–70. https://doi.org/10.1016/j.freeradbiomed.2023.01.014
12. DiMeo S, Reed TT, Venditti P, Victor VM. Role of ROS and RNS Sources in Physiological and Pathological Conditions. Oxid. Med. Cell Longev. 2016; 1245049. https://doi.org/10.1155/2016/1245049
13. Afzal S, Abdul Manap AS, Attiq A, Albokhadaim I, Kandeel M, Alhojaily SM. From imbalance to impairment: the central role of reactive oxygen species in oxidative stress-induced disorders and therapeutic exploration. Front. pharmacol. 2023; 14: 1269581. https://doi.org/10.3389/fphar.2023.1269581
14. Juan CA, Manuel J, Plou FJ. The Chemistry of Reactive Oxygen Species (ROS) Revisited: Outlining Their Role in Biological Macromolecules (DNA, Lipids and Proteins) and Induced Pathologies. Int. J. Mol. Sci. 2021; 22(9): 4642. https://doi.org/10.3390/ijms22094642
15. Pisoschi AM, Pop A. The role of antioxidants in the chemistry of oxidative stress: A review. Eur. J. Med. Chem. 2015; 97: 55–74. https://doi.org/10.1016/j.ejmech.2015.04.040
16. Han Y, Liu D, Cheng Y, Ji Q, Liu M, Zhang B, Zhou S. Maintenance of mitochondrial homeostasis for Alzheimer's disease: Strategies and challenges. Redox biol. 2023; 63: 102734. https://doi.org/10.1016/j.redox.2023.102734
17. Leyane TS, Jere SW, Houreld NN. Oxidative Stress in Ageing and Chronic Degenerative Pathologies: Molecular Mechanisms Involved in Counteracting Oxidative Stress and Chronic Inflammation. Int. J. Mol. Sci. 2022; 23(13): 7273. https://doi.org/10.3390/ijms23137273
18. Omran B, Baek KH. Nanoantioxidants: Pioneer Types, Advantages, Limitations, and Future Insights. Molecules. 2021; 26(22): 7031. https://doi.org/10.3390/molecules26227031
19. Flieger J, Flieger W, Baj J, Maciejewski R. Antioxidants: Classification, Natural Sources, Activity/Capacity Measurements, and Usefulness for the Synthesis of Nanoparticles. Materials. 2021; 14(15): 4135. https://doi.org/10.3390/ma14154135
20. Ashok A, Andrabi SS, Mansoor S, Kuang Y, Kwon BK, Labhasetwar V. Antioxidant Therapy in Oxidative Stress-Induced Neurodegenerative Diseases: Role of Nanoparticle-Based Drug Delivery Systems in Clinical Translation. Antioxidants. 2022; 11(2): 408. https://doi.org/10.3390/antiox11020408

21. Phaniendra A, Jestadi DB, Periyasamy L. Free radicals: properties, sources, targets, and their implication in various diseases. Indian J. Clin. Biochem. 2015; 30(1): 11–26. https://doi.org/10.1007/s12291-014-0446-0
22. Pham LA, He H, Pham-Huy C. Free Radicals, Antioxidants in Disease and Health. Int. J. Biomed. Sci. 2008; 4(2): 89-96. https://www.ncbi.nlm.nih.gov/pmc/articles/PMC3614697/
23. Shields HJ, Traa A, Van Raamsdonk JM. Beneficial and Detrimental Effects of Reactive Oxygen Species on Lifespan: A Comprehensive Review of Comparative and Experimental Studies. Front. Cell Dev. Biol. 2021; 9: 628157. https://doi.org/10.3389/fcell.2021.628157
24. Forman HJ, Zhang H. Targeting oxidative stress in disease: Promise and limitations of antioxidant therapy. Nat. Rev. Drug Discov. 2021; 20(9): 689-709. https://doi.org/10.1038/s41573-021-00233-1
25. Pisoschi AM, Pop A, Iordache F, Stanca L, Predoi G, Serban AI. Oxidative stress mitigation by antioxidants - An overview on their chemistry and influences on health status. Eur. J. Med. Chem. 2021; 209: 112891. https://doi.org/10.1016/j.ejmech.2020.112891
26. Tiwari MK, Mishra PC. Scavenging of hydroxyl, methoxy, and nitrogen dioxide free radicals by some methylated isoflavones. J. Mol. Model. 2018; 24(10): 287. https://doi.org/10.1007/s00894-018-3805-6
27. Choe E, Min DB. Mechanisms of Antioxidants in the Oxidation of Foods. Compr. Rev. Food Sci. Food Saf. 2009; 8(4): 345-358. https://doi.org/10.1111/j.1541-4337.2009.00085.x
28. Cynthya MM, Jun X, Abdul M, Suresh N, John, S. Antioxidant activity of polyphenols from Ontario grown onion varieties using pressurized low polarity water technology. J. Funct. Foods. 2017; 31: 52-62, https://doi.org/10.1016/j.jff.2017.01.037.
29. Brglez ME, Knez Hrncic M, Skerget M, Knez Z, Bren U. Polyphenols: Extraction Methods, Antioxidative Action, Bioavailability and Anticarcinogenic Effects. Molecules. 2016; 21(7): 901. https://doi.org/10.3390/molecules21070901
30. Debasis M, Debanjan M, Bensaad MS, Somya S, Kumud P, Manu P, Ankita P, Pallavi S, Saliha D, Leila H, Periyasamy P, Pradeep KDM. Evolution of bioinformatics and its impact on modern bio-science in the twenty-first century: Special attention to pharmacology, plant science and drug discovery. Comput. Toxicol. 2022; 24: 100248. https://doi.org/10.1016/j.comtox.2022.100248.
31. Makhouri FR, Ghasemi JB. In Silico Studies in Drug Research Against Neurodegenerative Diseases. Curr. Neuropharmacol. 2018; 16(6): 664–725. https://doi.org/10.2174/1570159X15666170823095628
32. Jia-Yun X, Kun W, Shu-Hui M, Yang Y, Quan Z, Zhen-Guang Y. QSAR-QSIIR-based prediction of bioconcentration factor using machine learning and preliminary application. Environ. Int. 2023; 177: 108003. https://doi.org/10.1016/j.envint.2023.108003.
33. Arkaprava B, Kunal R. Machine-learning-based similarity meets traditional QSAR: “q-RASAR” for the enhancement of the external predictivity and detection of prediction confidence outliers in an hERG toxicity dataset. Chemometr. Intell. Lab. Sys. 2023; 237: 104829. https://doi.org/10.1016/j.chemolab.2023.104829.
34. Babu S, Sohn H, Madhavan T. Computational Analysis of CRTh2 receptor antagonist: A Ligand-based CoMFA and CoMSIA approach. Comput. Biol. Chem. 2015; 56: 109–121. https://doi.org/10.1016/j.compbiolchem.2015.04.007
35. Wang F, Yang W, Zhou B. Studies on the antibacterial activities and molecular mechanism of GyrB inhibitors by 3D-QSAR, molecular docking and molecular dynamics

simulation. Arab. J. Chem. 2022; 15(6): 103872. https://doi.org/10.1016/j.arabjc.2022.103872
36. Abdizadeh R, Hadizadeh F, Abdizadeh T. QSAR analysis of coumarin-based benzamides as histone deacetylase inhibitors using CoMFA, CoMSIA and HQSAR methods. J. Mol. Struct. 2020; 1199: 126961. https://doi.org/10.1016/j.molstruc.2019.126961
37. Veríssimo GC, Menezes DEF, Teotonio Dias AL, deOliveira FP, Kronenberger T, Gomes MA, Maltarollo VG. HQSAR and random forest-based QSAR models for anti-T. vaginalis activities of nitroimidazoles derivatives. J. Mol. Graph. Model. 2019; 90: 180–191. https://doi.org/10.1016/j.jmgm.2019.04.007
38. Avwioroko OJ, Oyetunde TT, Atanu FO, Otuechere CA, Anigboro AA, Dairo OF, Ejoh AS, Ajibade SO, Omorogie MO. Exploring the binding interactions of structurally diverse dichalcogenoimidodiphosphinate ligands with α-amylase: Spectroscopic approach coupled with molecular docking. Biochem. Biophys. Rep. 2020; 24: 100837. https://doi.org/10.1016/j.bbrep.2020.100837
39. Fatima M, Bukhari MN, Chen S, Jiang L, Hashmi AA, Ahmad A, Bhatt IA, Ahmed S. Bioactivity and molecular docking of synthesized macromolecular ligand and its complex. Arab. J. Chem. 2020; 13(3): 4586-4593. https://doi.org/10.1016/j.arabjc.2019.09.009
40. Wang N, Wicht KJ, Imai K, Wang MQ, Anh Ngoc T, Kiguchi R, Kaiser M, Egan TJ, Inokuchi T. Synthesis, β-haematin inhibition, and in vitro antimalarial testing of isocryptolepine analogues: SAR study of indolo[3,2-c]quinolines with various substituents at C2, C6, and N11. Bioorg. Med. Chem. 2014; 22(9): 2629–2642. https://doi.org/10.1016/j.bmc.2014.03.030
41. Vilar S, Costanzi S. Predicting the biological activities through QSAR analysis and docking-based scoring. Methods Mol. Biol. 2012; 914: 271–284. https://doi.org/10.1007/978-1-62703-023-6_16
42. Shiri F, Pirhadi S, Ghasemi JB. Alignment independent 3D-QSAR, quantum calculations and molecular docking of Mer specific tyrosine kinase inhibitors as anticancer drugs. Saudi Pharm. J. 2016; 24(2): 197-212. https://doi.org/10.1016/j.jsps.2015.03.012
43. Kim H, Jeong H. Structure-Activity Relationship Studies Based on 3D-QSAR CoMFA/CoMSIA for Thieno-Pyrimidine Derivatives as Triple Negative Breast Cancer Inhibitors. Molecules. 2022; 27(22): 7974. https://doi.org/10.3390/molecules27227974
44. Hamad Elgazwy AS, Soliman DS, Atta-Allah SR, Ibrahim DA. Three-dimensional quantitative structure activity relationship (QSAR) of cytotoxic active 3,5-diaryl-4,5-dihydropyrazole analogs: a comparative molecular field analysis (CoMFA) revisited study. Chem. Cent. J. 2012; 6(1): 50. https://doi.org/10.1186/1752-153X-6-50
45. Dube PN, Mokale S, Datar P. CoMFA and docking study of 2,N6-disubstituted 1,2-dihydro-1,3,5-triazine-4,6-diamines as novel PfDHFR enzyme inhibitors for antimalarial activity. Bull. Fac. Pharm. Cairo Univ. 2014; 52(1): 125-134. https://doi.org/10.1016/j.bfopcu.2014.02.003
46. Gade S, Mahmood S. 3D-QSAR studies on CCR2B receptor antagonists: Insight into the structural requirements of (R)-3-aminopyrrolidine series of molecules based on CoMFA/CoMSIA models. J. Pharm. Bioallied Sci. 2012; 4(2): 123–133. https://doi.org/10.4103/0975-7406.94813
47. Ai Y, Wang ST, Sun PH, Song FJ. Combined 3D-QSAR modeling and molecular docking studies on pyrrole-indolin-2-ones as Aurora A kinase inhibitors. Int. J. Mol. Sci. 2011; 12(3): 1605–1624. https://doi.org/10.3390/ijms12031605

48. Zhao X, Chen M, Huang B, Ji H, Yuan M. Comparative Molecular Field Analysis (CoMFA) and Comparative Molecular Similarity Indices Analysis (CoMSIA) studies on α(1A)-adrenergic receptor antagonists based on pharmacophore molecular alignment. Int. J. Mol. Sci. 2011; 12(10): 7022–7037. https://doi.org/10.3390/ijms12107022
49. Balupuri A, Balasubramanian PK, Cho SJ. 3D-QSAR, docking, molecular dynamics simulation and free energy calculation studies of some pyrimidine derivatives as novel JAK3 inhibitors. Arab. J. Chem. 2020; 13(1): 1052-1078. https://doi.org/10.1016/j.arabjc.2017.09.009
50. Sharma MC, Jain S, Sharma R. In silico screening for identification of pyrrolidine derivatives dipeptidyl peptidase-IV inhibitors using COMFA, CoMSIA, HQSAR and docking studies. In silico pharmacol. 2017; 5: 13. https://doi.org/10.1007/s40203-017-0032-2
51. Vyas VK, Ghate M, Gupta N. 3D QSAR and HQSAR analysis of protein kinase B (PKB/Akt) inhibitors using various alignment methods. Arab. J. Chem. 2017; 10: S2182-S2195. https://doi.org/10.1016/j.arabjc.2013.07.052
52. Fang Y, Lu Y, Zang X, Wu T, Qi X, Pan S, Xu X. 3D-QSAR and docking studies of flavonoids as potent Escherichia coli inhibitors. Sci. Rep. 2016; 6(1): 1-13. https://doi.org/10.1038/srep23634
53. Tian Y, Tong J, Liu Y, Tian Y. QSAR Study, Molecular Docking and Molecular Dynamic Simulation of Aurora Kinase Inhibitors Derived from Imidazo[4,5-b]pyridine Derivatives. Molecules. 2024; 29(8): 1772. https://doi.org/10.3390/molecules29081772
54. Aouidate A, Ghaleb A, Ghamali M, Chtita S, Ousaa A, Choukrad M, Sbai A, Bouachrine M, Lakhlifi T. Computer aided drug design based on 3D-QSAR and molecular docking studies of 5-(1H-indol-5-yl)-1,3,4-thiadiazol-2-amine derivatives as PIM2 inhibitors: a proposal to chemists. In silico pharmacol. 2018; 6(1): 5. https://doi.org/10.1007/s40203-018-0043-7
55. Garcia ML, Bueno RV, R.Nogueira VH, C.Guido RV. QSAR studies on benzothiophene derivatives as Plasmodium falciparum N-myristoyltransferase inhibitors: Molecular insights into affinity and selectivity. Drug Dev. Res. 2022; 83(2): 264-284. https://doi.org/10.1002/ddr.21646
56. Kimand SK, Jacobson KA. Three-dimensional quantitative structure-activity relationship of nucleosides acting at the A3 adenosine receptor: analysis of binding and relative efficacy. J. Chem. Inf. Model. 2007; 47(3): 1225–1233. https://doi.org/10.1021/ci600501z
57. Halder AK, Cordeiro MNDS. AKT Inhibitors: The Road Ahead to Computational Modeling-Guided Discovery. Int. J. Mol. Sci. 2021; 22(8): 3944. https://doi.org/10.3390/ijms22083944
58. Sharma R, Patil S, Maurya P. Drug discovery studies on quinoline-based derivatives as potential antimalarial agents. SAR QSAR Environ. Res. 2014; 25(3): 189–203. https://doi.org/10.1080/1062936X.2013.875484
59. Joshi D, Yadav S, Sharma R, Pandya M, Bhadauria RS. Molecular Modelling Studies on Thiazole-Based α-Glucosidase Inhibitors Using Docking and CoMFA, CoMSIA and HQSAR. Curr. Drug Discov. Technol. 2021; 18(6): e130921187100. https://doi.org/10.2174/1570163817666201022111213
60. Aziz AN, Taha M, Ismail NH, Anouar H, Yousuf S, Jamil W, Awang K, Ahmat N, Khan KM, Kashif SM. Synthesis, crystal structure, DFT studies and evaluation of the antioxidant activity of 3,4-dimethoxybenzenamine schiff bases. Molecules. 2014; 19(6): 8414–8433. https://doi.org/10.3390/molecules19068414

61. Sridhar J, Foroozesh M, Stevens CL. QSAR models of cytochrome P450 enzyme 1A2 inhibitors using CoMFA, CoMSIA and HQSAR. SAR QSAR Environ. Res. 2011; 22(7-8): 681–697. https://doi.org/10.1080/1062936X.2011.623320
62. Song Z, Qiao J, Tian D, Dai M, Guan Q, He Y, Liu P, Shi J. Glutamic acid can prevent the browning of fresh-cut potatoes by inhibiting PPO activity and regulating amino acid metabolism. LWT. 2023; 180: 114735. https://doi.org/10.1016/j.lwt.2023.114735
63. Santi MD, Bouzidi C, Gorod NS, Puiatti M, Michel S, Grougnet R, Ortega MG. In vitro biological evaluation and molecular docking studies of natural and semisynthetic flavones from Gardenia oudiepe (Rubiaceae) as tyrosinase inhibitors. Bioorg. Chem. 2019; 82: 241–245. https://doi.org/10.1016/j.bioorg.2018.10.034
64. Ghalla H, Issaoui N, Bardak F, Atac A. Intermolecular interactions and molecular docking investigations on 4-methoxybenzaldehyde. Comput. Mater. Sci. 2018; 149: 291-300. https://doi.org/10.1016/j.commatsci.2018.03.042
65. Gupta AK, Bhunia SS, Balaramnavar VM, Saxena AK. Pharmacophore modelling, molecular docking and virtual screening for EGFR (HER 1) tyrosine kinase inhibitors. SAR QSAR Environ. Res. 2011; 22(3): 239–263. https://doi.org/10.1080/1062936X.2010.548830
66. Bergman J, Engqvist R, Stalhandske CI, Wallberg H. Studies of the reactions between indole-2,3-diones (isatins) and 2-aminobenzylamine. Tetrahedron. 2003; 59(7): 1033-1048. https://doi.org/10.1016/S0040-4020(02)01647-2
67. Anwar A, Hameed A, Perveen S, Uroos M, Choudhary MI, Basha FZ. 1,1-Diphenyl-2-picrylhydrazyl radical scavenging activity of novel dihydropyridine derivatives. Eur. J. Chem. 2014; 5(1): 189-191. http://doi.org/10.5155/eurjchem.5.1.189-191.916
68. Baliyan S, Mukherjee R, Priyadarshini A, Vibhuti A, Gupta A, Pandey RP, Chang CM. Determination of Antioxidants by DPPH Radical Scavenging Activity and Quantitative Phytochemical Analysis of *Ficus religiosa*. Molecules. 2022; 27(4): 1326. https://doi.org/10.3390/molecules27041326
69. Kaddouri Y, Abrigach F, Yousfi EB, ElKodadi M, Touzani R. New thiazole, pyridine and pyrazole derivatives as antioxidant candidates: synthesis, DFT calculations and molecular docking study. Heliyon, 2020; 6(1): e03185. https://doi.org/10.1016/j.heliyon.2020.e03185
70. Gulcin I. Fe^{3+}–Fe^{2+} Transformation Method: An Important Antioxidant Assay. In: Armstrong, D. (eds) Advanced Protocols in Oxidative Stress III. Methods in Molecular Biology, Humana Press, New York, 2015; Vol. 1208, pp. 233-246. https://doi.org/10.1007/978-1-4939-1441-8_17
71. Benzie IF, Strain JJ. The ferric reducing ability of plasma (FRAP) as a measure of "antioxidant power": the FRAP assay. Anal. Biochem. 1996; 239(1): 70–76. https://doi.org/10.1006/abio.1996.0292
72. Ozyurek M, Bektasoglu B, Guclu K, Gungor N, Apak R. A novel hydrogen peroxide scavenging assay of phenolics and flavonoids using cupric reducing antioxidant capacity (CUPRAC) methodology. J. Food Compos. Anal. 2010; 23(7): 689-698. https://doi.org/10.1016/j.jfca.2010.02.013
73. Alam MN, Bristi NJ, Rafiquzzaman M. Review on in vivo and in vitro methods evaluation of antioxidant activity. Saudi Pharm. J. 2013; 21(2): 143-152. https://doi.org/10.1016/j.jsps.2012.05.002

74. Kumar RS, Rajkapoor B, Perumal P. Antioxidant activities of Indigofera cassioides Rottl. Ex. DC. using various in vitro assay models. Asian Pac. J. Trop. Biomed. 2012; 2(4): 256–261. https://doi.org/10.1016/S2221-1691(12)60019-7

75. Kumar V, Mathela C, Kumar M, Tewari G. Antioxidant potential of essential oils from some Himalayan Asteraceae and Lamiaceae species. Med. Drug Discov. 2019; 1: 100004. https://doi.org/10.1016/j.medidd.2019.100004

76. Lalhminghlui K, Jagetia GC. Evaluation of the free-radical scavenging and antioxidant activities of Chilauni, *Schima wallichii* Korth *in vitro*. Fut. Sci. OA. 2018; 4(2): 272. https://doi.org/10.4155/fsoa-2017-0086

77. Morales-Ubaldo AL, Rivero-Perez N, Valladares-Carranza B, Madariaga-Navarrete A, Higuera-Piedrahita RI, Delgadillo-Ruiz L, Banuelos-Valenzuela R, Zaragoza-Bastida A. Phytochemical Compounds and Pharmacological Properties of *Larrea tridentata*. Molecules. 2022; 27(17): 5393. https://doi.org/10.3390/molecules27175393

78. Saghaie L, Pourfarzam M, Fassihi A, Sartippour B. Synthesis and tyrosinase inhibitory properties of some novel derivatives of kojic acid. Research pharma. Sci. 2013; 8(4): 233–242. PMCID: PMC3757588

79. Zengin G, Mahomoodally M, Picot-Allain C, Cakmak Y, Uysal S, Aktumsek A. In vitro tyrosinase inhibitory and antioxidant potential of Consolida orientalis, Onosma isauricum and Spartium junceum from Turkey. S. Afr. J. Bot. 2019; 120: 119-123. https://doi.org/10.1016/j.sajb.2018.01.010

80. Piao LZ, Park HR, Park YK, Lee SK, Park JH, Park MK. Mushroom tyrosinase inhibition activity of some chromones. Chem. Pharm. Bull. 2002; 50(3): 309–311. https://doi.org/10.1248/cpb.50.309

81. Athipornchai A, Niyomtham N, Pabuprapap W, Ajavakom V, Duca M, Azoulay S, Suksamrarn A. Potent Tyrosinase Inhibitory Activity of Curcuminoid Analogues and Inhibition Kinetics Studies. Cosmetics. 2021; 8(2): 35. https://doi.org/10.3390/cosmetics8020035